Magnetic behavior of $R_2Cu_2O_5$ cuprates studied by neutron diffraction

J. L. García-Muñoz and X. Obradors
Institut de Ciència de Materials de Barcelona, Consejo Superior de Investigaciones Científicas, Campus Universitat Autònoma de Barcelona, ES-08193 Bellaterra, Spain

J. Rodríguez-Carvajal
Institut Laue-Langevin, 38042 Grenoble-Cedex, France
(Received 8 September 1994; revised manuscript received 23 November 1994)

We report the results of an extensive neutron-diffraction study on the magnetic properties of the $R_2Cu_2O_5$ family of cuprates, with R = Y, Er, Tm, Ho, and Yb. The magnetic structures at 1.5 K have been determined in all cases, ruling out some models previously proposed. In most cases Cu sites show a similar relative magnetic arrangement: ferromagnetic chains parallel to the a axis, ferromagnetically or antiferromagnetically coupled along b in the ab plane. The easy axis of the $S=\frac{1}{2}$ spins varies from one compound to another. The arrangement of the R moments differs strongly between the different compounds, indicating competition between the crystal field and R-Cu exchange interactions. The magnetic moments of the rare earth are polarized under the local effective field from ordered Cu spins, the R-R interactions being negligible. The low-temperature magnetic order in $Ho_2Cu_2O_5$ and $Yb_2Cu_2O_5$ does not occur simultaneously in Cu and R sublattices. The intermediate transitions observed in $Ho_2Cu_2O_5$ and $Yb_2Cu_2O_5$ (incommensurate) indicate competition and unsatisfied interactions between copper and rare-earth sublattices. In these compounds the propagation vector seems to express the degree of frustration in the structure. In $Yb_2Cu_2O_5$, Yb moments frozen well below Cu spins through a first-order transition that also involves the transformation of the incommensurate order of Cu spins into the final $\mathbf{k}=(0,\frac{1}{2},\frac{1}{2})$ magnetic structure.

I. INTRODUCTION

The interplay between rare-earth magnetic ordering and Cu ions in superconducting or antiferromagnetic cuprates is being widely investigated in the framework of the subtle relationship between magnetism and superconductivity. The magnetic properties of rare-earth ions (R) in $RBa_2Cu_3O_6$ and R_2CuO_4 compounds and their doped superconducting versions are being used as a probe of the magnetic interactions between copper moments, relevant for the observation of superconductivity.[1–4] In most cases, the high Néel temperatures of the rare-earth ions are indicative of a $4f$ and CuO_2 superexchange mechanism. In $Sm_{2-x}A_xCuO_4$ ($A=Ce^{4+}$ or Y^{3+}), for instance, Ce^{4+} substitution suppresses the Sm^{3+} Néel temperature much more effectively that Y^{3+} substitution, suggesting that the insertion of carriers into the CuO_2 planes affects the Sm^{3+} ordering.[5] Many of these results are actually interpreted by invoking models where covalent bonding of the rare earths to neighboring oxygens leads to a superexchange interaction.[6] On another hand the effects of anisotropy in the puzzling behavior of the rare-earth sublattices are not well understood yet in these cuprates.

In the ternary R-Cu-O phase diagram, the orthorhombic La_2CuO_4-type structure (T) is substituted by the T' type, with Cu in square-planar coordination, for small rare earths (from Pr to Gd). The metastable T^* structure occurs in a very narrow region at the T/T' boundary, resulting from a thermodynamic competition between T and T' structures. Finally, the R_2CuO_4 composition is no longer stable at atmospheric pressure for rare earths smaller than Gd. Then, the $R_2Cu_2O_5$ crystal structure arises for the heavier rare earths. The segregation of the T, T^*, T' and $R_2Cu_2O_5$ phases[7] is accompanied by systematic changes of the oxygen coordination of the rare earth as its size decreases: ninefold coordination in T, eightfold in T' and sixfold in $R_2Cu_2O_5$. This last family of cuprates represents, in this context, an opportunity to further increase our understanding of the role of the copper sublattices and the R-Cu exchange interactions in the magnetic ordering of the rare earths.

In this paper we present the results of systematic neutron-scattering studies of the three-dimensional magnetism in $R_2Cu_2O_5$ compounds with R = Y, Er, Tm, Ho, and Yb. The magnetic features found make these compounds interesting in their own right. In a previous paper[8] we briefly reported their magnetic structures at 1.5 K. In the present work we give more extensive details about the magnetic transitions in these oxides, the implications of the magnetic ordering to the metamagnetic like transitions previously observed,[9] and detailed information concerning the behavior of copper and rare-earth sublattices as they achieve magnetic ordering. The magnetic behavior of these cuprates includes commensurate and incommensurate reorientations of copper sublattices; proves the importance of Cu-Cu and R-Cu interactions for rare-earth magnetic ordering, and, in some cases, the existence of strong competition and frustrated interactions between copper and rare-earth sublattices.

II. EXPERIMENTAL DETAILS

The polycrystalline samples were synthesized by solid-state reaction from oxides in air. Following the method of sample preparation described in Ref. 10, $R_2Cu_2O_5$ samples were obtained with R = Y, Er, Tm, Ho, and Yb. These samples were investigated by means of neutron diffraction at the Institut Laue Langevin in Grenoble; we used the D2B high-resolution powder diffractometer ($\lambda \approx 1.59$ Å) in its high flux mode of operation at low (1.5 K) and room temperatures (RT). The step size for the measurements was 0.05° and the angular range 0°–160° (2Θ). The evolution of the magnetic intensities with temperature was monitored (in 1-K steps) on the high flux D1B ($\lambda \approx 2.52$ Å) diffractometer. This instrument is equipped with a position sensitive detector spanning 80° in 2Θ. For the low-temperature range, a vanadium can with the sample inside was placed in a helium "orange" cryostat. $Y_2Cu_2O_5$ and $Er_2Cu_2O_5$ were also measured on D20 ($\lambda = 2.42$ Å) at 1.5 K and studied by ac susceptibility and magnetization measurements in a vibrating sample magnetometer, and intense magnetic field measurements up to 20 T at the Service National des Champs Intenses in Grenoble.

The diffraction data were analyzed by the Rietveld method by use of the program FULLPROF.[11] A very small amount of R_2O_3 was detected in some cases and included as impurity phase ($R_2O_3 \lesssim \approx 3.6\%$). The data obtained on D2B at RT were analyzed first in order to thoroughly study the details of the nuclear structure. The atomic coordinates and relevant crystallographic parameters are not included in the present work since they have been gathered in Refs. 12 and 13. In Ref. 13 we reported a detailed discussion of the $R_2Cu_2O_5$ structures.

III. RESULTS AND DISCUSSION

The method followed for the determination of the magnetic structures that appear at low temperatures was thoroughly described in Ref. 8. Consequently it is not repeated here again. It is worthwhile remembering that there exist four different magnetic sites (two of copper and two of rare earth), each with multiplicity four. The magnetic structures at 1.5 K are gathered in Table I, the symbol used for their description are based in the following sequence of signs for the atoms 1, 2, 3, and 4 (see Refs. 8, 14, and 15): $F(++++)$, $G(+-+-)$, $C(++--)$, and $A(+--+)$.

The numbering of the four equivalent sublattices ($1 \rightarrow 4$) is displayed in Fig. 3(b) and their coordinates given in Ref. 8. Figure 1 shows the observed and calculated neutron-diffraction patterns of $Er_2Cu_2O_5$, $Ho_2Cu_2O_5$, and $Yb_2Cu_2O_5$ at 1.5 K, by considering the magnetic ordering summarized, respectively, in Table I (see also Ref. 8).

A. $Y_2Cu_2O_5$ and $Er_2Cu_2O_5$

In agreement with Ref. 8, Cu moments in $Er_2Cu_2O_5$ order as in $Y_2Cu_2O_5$ (Fig. 2), with ferromagnetic Cu ab pseudolayers stacked antiparallel along the c axis. It is to be noted that in $Er_2Cu_2O_5$ the magnetic arrangement of both Cu and Er moments can be described by the basis functions of the same representation: $[G_x, A_y, C_z]$ (Table I), the Cu sublattices with null x and z components. This is a significant indication of an important coupling between copper and rare-earth sublattices, consistent with the simultaneous ordering of both ions, and with an effective Hamiltonian in which the $J_{\text{Er-Cu}}$ interaction is one of the leading terms. As pointed out in Ref. 8, the pseudolayers of Cu moments are bracketed by two Er layers to which the first are antiferromagnetically (AF) coupled [Fig. 3(a)]. In Sec. III B we will show that the high T_N of $Er_2Cu_2O_5$, compared to the other rare earths, is not due to a stronger R-Cu exchange but, mainly, to the large Er moment.

Cheong *et al.*[19] reported a complex metamagnetic behavior in $Y_2Cu_2O_5$ (single crystal) when the applied

TABLE I. Magnetic structure at 1.5 K of $R_2Cu_2O_5$. (a) Wave vector and modes. (b) Reference moments in μ_B; in double signs ($\pm$) refer to the two different sites.

(a)

	Y	Er	Tm	Ho	Yb
T_N (K)	13	28	17	13/7.4	13/8
k	(000)	(000)	(000)	$(0\,\frac{1}{2}\,0)$	$(0\,\frac{1}{2}\,1/2)$
Cu(1)	A_y	A_y	$(-A_x)$	F_z	A_y
Cu(2)	A_y	A_y	A_x	F_z	A_y
$R(1)$		$G_x(-A_y)C_z$	$A_x(-F_z)$	$(-G_x)A_yC_z$	A_xG_y
$R(2)$		$G_x(-A_y)(-C_z)$	$A_x(-F_z)$	$(-G_x)A_yC_z$	$(-A_x)G_y$

(b)

	R					Cu				
	m_x	m_y	m_z	m_T	$m_{\text{free ion}}$	m_x	m_y	m_z	m_T	$m_{\text{free ion}}$
Y							1.1(1)		1.1(1)	[1]
Er	0.7(1)	−5.5(1)	±2.9(1)	6.2(1)	[9]		1.2(1)		1.2(1)	[1]
Tm	2.6(1)		−3.0(1)	4.0(1)	[7]	−0.9(1)			0.9(1)	[1]
Ho	−4.3(1)	0.9(1)	7.7(1)	9.0(1)	[10]			0.8(2)	0.8(2)	[1]
Yb	±0.6(1)	1.2(1)		1.4(1)	[4]		1.1(1)		1.1(1)	[1]

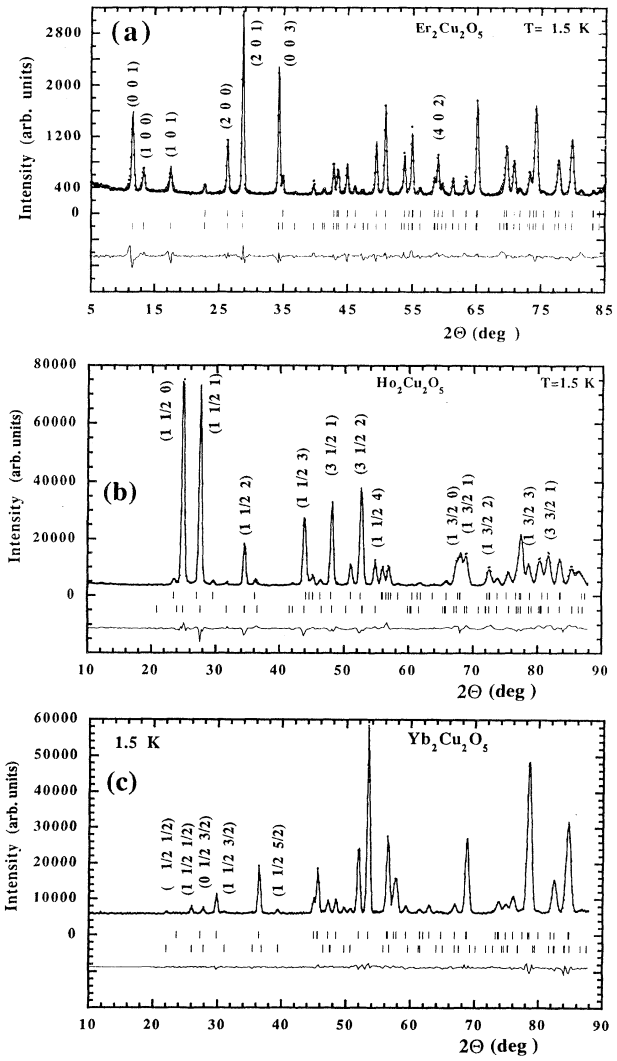

FIG. 1. Observed (+) and calculated (−) neutron-diffraction patterns at 1.5 K of (a) $Er_2Cu_2O_5$, (b) $Ho_2Cu_2O_5$, and (c) $Yb_2Cu_2O_5$. The second row of reflection markers corresponds to the magnetic reflections.

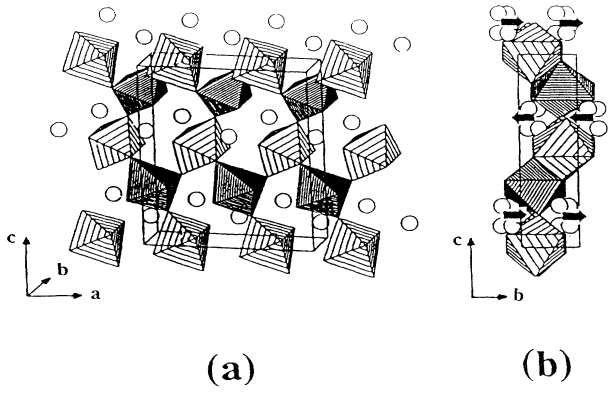

FIG. 2. (a) Representation of the $R_2Cu_2O_5$ structure showing the RO_6 octahedra. (b) Projection of the structure showing the AF coupling of the ferromagnetic Cu-O pseudolayers in $Y_2Cu_2O_5$.

magnetic field is parallel to the b axis (easy axis). At 2 K, two magnetization steps are observed up to 5 T: the first of $\approx 0.3\mu_B$/Cu ion and the second was incomplete below that field. In Ref. 8 we proposed that only one chain in a tripled cell flips their moments in the first transition. Figure 4(a) represents the magnetization at 4 K of $Y_2Cu_2O_5$ up to intense fields. Saturation of the magnetization is reached above $H \approx 11$ T. The magnetization $M_S = 29.0$ emu/g corresponds to all the Cu spins aligned. Thus, the confirmation of only two field-induced transitions before saturation reinforces the idea that the two remaining inverted chains in the inset of Fig. 4(a) flip their spins in the second transition. On another hand, in addition to the magnetization jump reported in Ref. 9 for $Er_2Cu_2O_5$ (from which a proposed model for the transition can be found in Ref. 8), Fig. 4(b) reveals a second induced transition at 14 T in this same compound. This metamagnet-

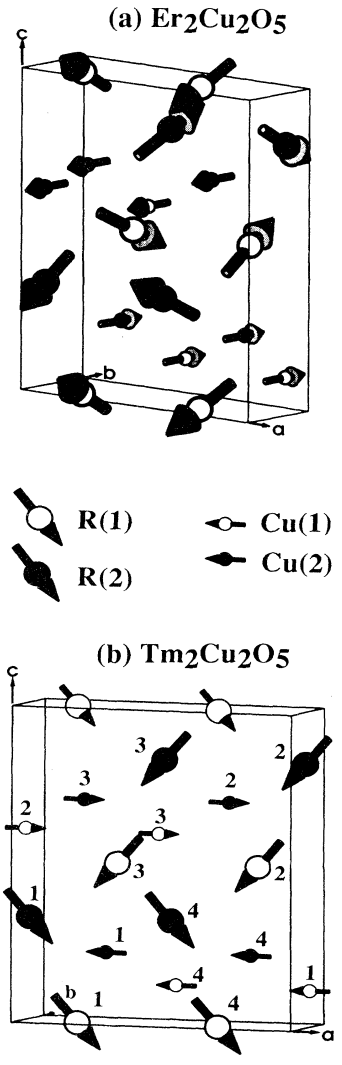

FIG. 3. Magnetic structure of (a) $Er_2Cu_2O_5$, and (b) $Tm_2Cu_2O_5$, both having null propagation vector ($\mathbf{k}=0$). The values of magnetic moment components at 1.5 K are given in Table I.

iclike behavior deserves further investigations with single crystals.

B. Net canted Tm ferromagnetism in $Tm_2Cu_2O_5$

The magnetic structure of $Tm_2Cu_2O_5$ is shown in Fig. 3(b). As in $(Y,Er)_2Cu_2O_5$ copper moments are aligned ferromagnetically in the *ab* plane and are AF arranged to the adjacent *ab* pseudolayers. However, the likely AF Cu^{2+}-Tm^{3+} interaction forces the Cu^{2+} moments in $Tm_2Cu_2O_5$ to rotate from *b* to *a* axis with respect to $Y_2Cu_2O_5$. In addition, there is a canted ferromagnetic arrangement of Tm moments. Tm(1) and Tm(2) sublattices exhibit the same magnetic structure ($\{A_x 0 F_z\}$) with parallel moments at the same site ($1 \rightarrow 4$). Apparently, the direction of the Tm moments is fixed by the crystal field anisotropy, and $J_{\text{Tm-Cu}}$ exchange forces the $S=\frac{1}{2}$ Cu^{2+} spins to point parallel to *a*, while they point parallel to *b* in $Y_2Cu_2O_5$ and $Er_2Cu_2O_5$. The net ferromagnetic component F_z of Tm explains the magnetization and susceptibility measurements by Troc *et al.*,[10] and the absence of induced transitions on powder samples of this cuprate.[9]

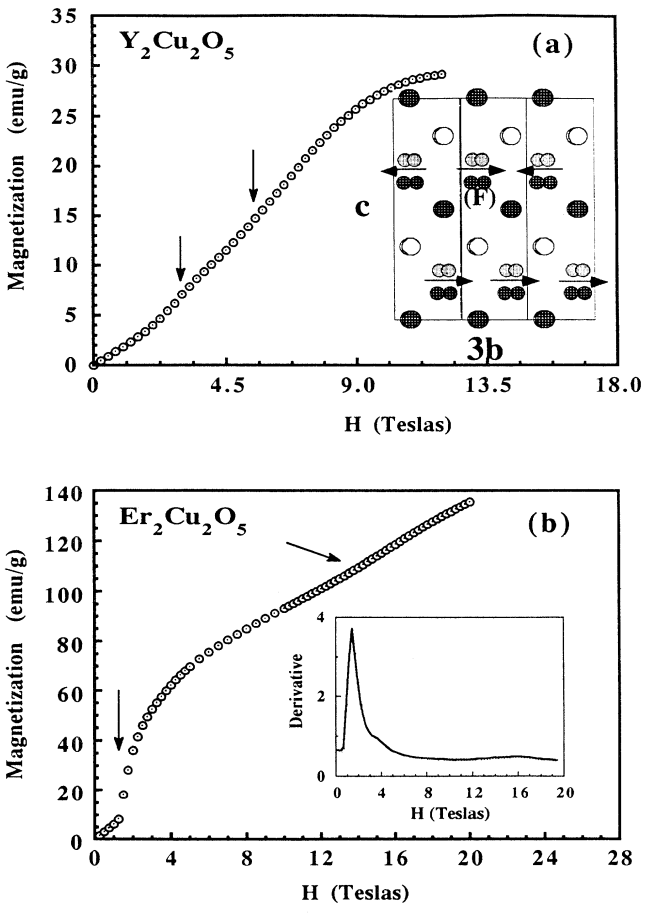

FIG. 4. Magnetization curves at 4.2 K of (a) $Y_2Cu_2O_5$ and proposed magnetic order after the first field-induced transition ["(*F*)" marks the flipped **m**]; and (b) $Er_2Cu_2O_5$, up to 20 T, showing the two induced transitions.

The thermal dependence of the ordered rare-earth moments is very different from the Brillouin-type, as followed by m(Cu) [see Fig. 5(a)]. In the inset of this figure the evolution of the normalized moments $m_R(T)/m_R(0)$ with R=Tm and Er are compared as a function of the reduced temperature ($\tau = T/T_N$). Their almost identical

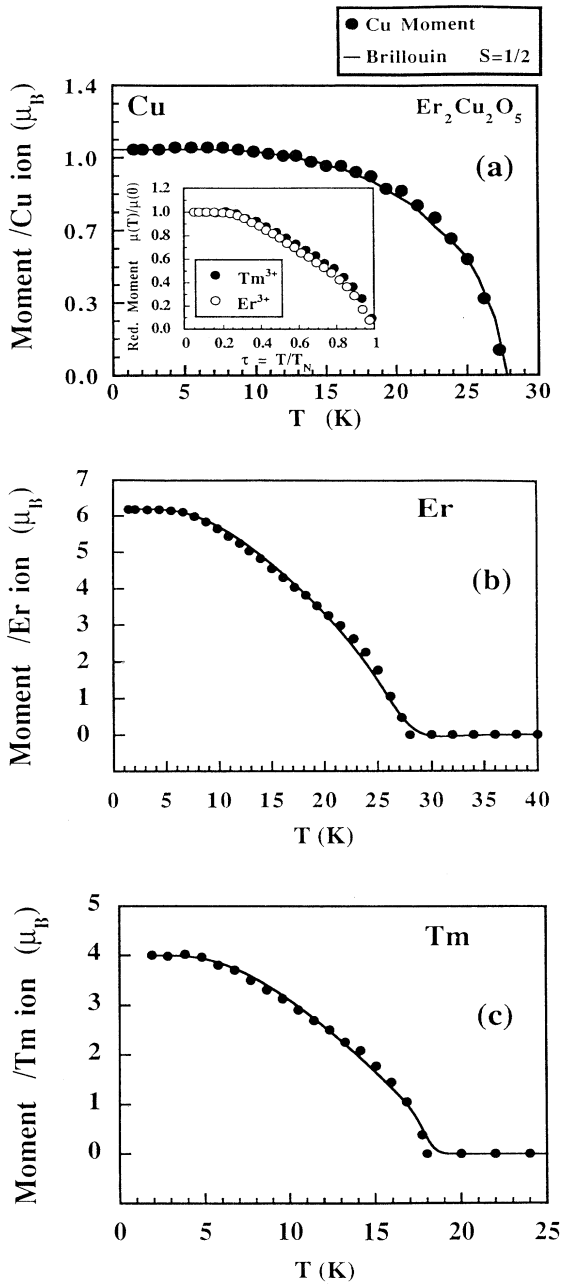

FIG. 5. (a) Temperature evolution of m(Cu) in $Er_2Cu_2O_5$. Inset: comparison of the evolution with temperature of the normalized R ordered moments in $Er_2Cu_2O_5$ and $Tm_2Cu_2O_5$. In the figure, the reduced temperature $\tau = T/T_N$ has been considered. Calculated R moments in (b) $Er_2Cu_2O_5$ and (c) $Tm_2Cu_2O_5$ from the effective molecular field created by the ordered Cu spins as a function of temperature (see explanation in the text).

behavior is consistent with $S=\frac{1}{2}$ Cu spins defining essentially the exchange field responsible for the ordering of rare-earth moments.

We have used a simple model to reproduce the behavior of $m_R(T)$ that basically only regards the R-Cu magnetic exchange interaction. By considering a ground and first excited state as the only crystal-field active levels[16] the ordered moment per rare-earth ion is given by[17]

$$m_R(T,H_{\rm loc})=\mu_R\tanh(\mu_R H_{\rm loc}/kT)\ , \tag{1}$$

where μ_R is the saturation magnetic moment of the rare earth in units of μ_B. We have expressed the local field seen by the R^{3+} ion, $H_{\rm loc}$, as

$$H_{\rm loc}(T)=\left|\sum_i^n \lambda_i \mathbf{m}_i(T)\right|=\lambda m_{\rm Cu}(T)\ , \tag{2}$$

where the direct R-R interaction is disregarded, and λ_i coefficients are proportional to the effective R-Cu exchange integrals ($\lambda_i=2J^i_{R\text{-Cu}}/(g\mu_B)^2\approx\lambda/n$) with neighbor Cu ions. $m_{\rm Cu}(T)$ is the thermal average of Cu moments [represented in Fig. 5(a) for $Er_2Cu_2O_5$]. The evolution of $m_{\rm Cu}(T)$ is identical in $Y_2Cu_2O_5$ and $Er_2Cu_2O_5$ and $Tm_2Cu_2O_5$ when the reduced temperature τ is considered.

By fitting the single parameter λ, in kOe/μ_B, we have reproduced the experimental evolution of $m_{\rm Tm}(T)$ and $m_{\rm Er}(T)$. They are compared to the calculated values in Figs. 5(b) and 5(c). The molecular field Cu-R exchange constant $\lambda_{R\text{-Cu}}$ is 34 kOe/μ_B with R = Er and 38 kOe/μ_B in the Tm compound. (In Ref. 18, $\lambda_{\text{Er-Cu}}$ was determined to be 44 kOe/μ_B from an optical spectroscopy study.) These similar values should be compared to the equivalent molecular-field parameter

$$\left[\lambda_{\text{Cu-Cu}}=\frac{3kT_N}{S(S+1)(g\mu_B)^2}\approx 2z\,|J_{\text{Cu-Cu}}|\right]$$

in $Y_2Cu_2O_5$ (T_N = 11 K), $\lambda_{\text{Cu-Cu}}\approx 135$ kOe/μ_B.[12] Therefore, $\lambda_{\text{Cu-Cu}}/\lambda_{R\text{-Cu}}\approx 3.8$.

C. $Ho_2Cu_2O_5$: towards competition between sublattices

Several works have been published devoted to the magnetic structure of $Ho_2Cu_2O_5$, with significant differences among them. We have carefully examined all the proposed models by comparison with our neutron data from high flux measurements. The propagation vector is $\mathbf{k}=(0,\frac{1}{2},0)$, and hence the magnetic cell is doubled along the b axis. We confirm the magnetic structure of Ho moments described by $(-G_x)A_yC_z$, in agreement with Refs. 8, 20, and 21. With a small but non-null m_y(Ho) component.

In this magnetic structure, Ho moments at the same ab plane are basically AF coupled, while moments in adjacent R planes are noncollinear. As shown in Fig. 6(a), the copper pseudolayers are bracketed by Ho layers with identical moment alignment. The accurate values of the moments are given in Table I. The magnetic model proposed by Andresen, Golab, and Szytula[22] from neutron data at 9 K is essentially the same, but they deal with a G_y mode along b that leads to a poorer magnetic R factor. Moreover, the direction given for Ho moments in Ref. 22 is only approximate. Finally, our structure factor calculations gave wrong intensities for the $(0\,\frac{1}{2}\,1)$ reflections with the model reported in Ref. 23.

Because of the large moment of $Ho^{3+}(4f^{10},{}^5I_8)$, it was not easy to discern the behavior of Cu atoms. Their ordering was confirmed by the presence of some weak reflections, such as the $(0\,\frac{1}{2}\,2)$, clearly associated (from simulations) to ordered moments at the copper sublattices. The arrangement of the $S=\frac{1}{2}$ Cu spins that better reproduces the experimental intensities is the mode F_z [for Cu(1) and Cu(2) sublattices, model (b) in Ref. 20]. The (a) and (c) possible magnetic structures also given in Ref. 20 lead to a very slightly worse magnetic R factor ($R_{\rm Mag}=5.1\%$ vs 4.5%). The main component of Ho is also m_Z. Because of the propagation vector $\mathbf{k}=(0,\frac{1}{2},0)$ the copper pseudolayer are no longer ferromagnetic [see Fig. 3(c)]. The ab pseudoplanes of copper are constituted by F chains perpendicular to b and alternatively inverted, in contrast with the ferromagnetic disposition in the pre-

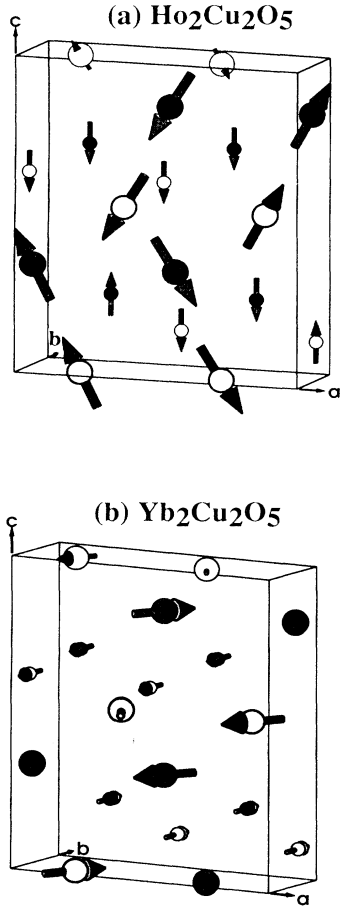

FIG. 6. Magnetic structure at 1.5 K of (a) $Ho_2Cu_2O_5$, and (b) $Yb_2Cu_2O_5$. The magnetic structure has been represented within the crystallographic unit cell. Spins in adjacent cells are inverted according to the propagation vector $\mathbf{k}=(0,\frac{1}{2},0)$ (for Ho), and $\mathbf{k}=(0,\frac{1}{2},\frac{1}{2})$ (for Yb). The values of magnetic moment components at 1.5 K are given in Table I.

vious compounds. Probably, the doubled periodicity along b arises from the competition between the crystal-field anisotropy of Ho and the Ho-Cu exchange interaction. By doubling the periodicity the system seems to achieve a configuration of compromise.

In addition, the thermal evolution of the diffracted intensities around the most intense magnetic reflections [$(1\,\frac{1}{2}\,0)$ and $(1\,\frac{1}{2}\,1)$] reveals short-range magnetic order (SRO) up to $T_{SRO}\approx 3T_N$ ($\approx$25 K above $T_N=13$ K). The existence of such $\langle \mathbf{m}_i^k[\mathrm{Ho}]\cdot\mathbf{m}_j^k[\mathrm{Ho}]\rangle$ SRO correlations already with $\mathbf{k}=(0,\frac{1}{2},0)$ below $T\approx 40$ K is probably the consequence of important low-dimensional correlations in the Cu subsystem well above T_N.

Even more, the competition between sublattices brings about interesting phenomena in $Ho_2Cu_2O_5$ (and $Yb_2Cu_2O_5$) before the final magnetic order is achieved. Our data reveal two different ordered magnetic regimes in $Ho_2Cu_2O_5$ that are separated by an intermediate spin reorientation of copper at $T_{N1}\approx 7.4$ K. The two transition temperatures in these cuprates are $T_{N1}\approx 7.4$ K and $T_{N2}\approx 13$ K. In Fig. 7 has been represented the thermal evolution of the diffracted intensities at low angles. The intensity of the magnetic reflection $(0\,\frac{1}{2}\,0)$ is only apparent in the interval $7.4\text{ K}<T<13$ K. And practically vanishes below T_{N1}, coinciding with the emergence of the $(0\,\frac{1}{2}\,2)$ reflection (not visible in Fig. 7) and the final spin ordering described above. We verified that the intensity at $(0\,\frac{1}{2}\,0)$ strongly depends on the arrangement of Cu spins, and the intermediate spin reorientation is essentially related to a change in the arrangement of copper moments. Even if the magnetic structure of Ho is probably unmodified, the smallness of the intensity changes does not allow us to discern the exact ordering in the copper sublattices below T_{N2}. These moments seem to be nonsaturated above the low transition temperature T_{N1}, and, clearly, their periodicity is also doubled along b. Complementary measurements on single crystals are desirable in this temperature range. We think that the low transition temperatures, compared to the rest (in spite of the large Ho moment) and the non-null propagation vector are indicative of frustrated interactions in $Ho_2Cu_2O_5$. In this way, the consequences of competing interactions are much more dramatic in $Yb_2Cu_2O_5$.

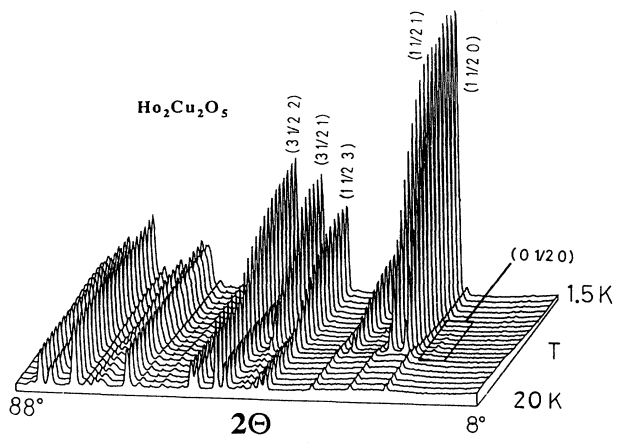

FIG. 7. Temperature dependence of the small-angle neutron-diffraction reflections of $Ho_2Cu_2O_5$. Apart from the main magnetic reflections the figure illustrates the presence of the very weak magnetic reflection $(0\,\frac{1}{2}\,0)$ within the interval $T_{N1}\approx 7.4\text{ K}\le T\le T_{N2}\approx 13$ K. At T_{N1} this intensity vanishes and the $(0\,\frac{1}{2}\,2)$ reflection emerges (see explanation in the text).

D. $Yb_2Cu_2O_5$: effects of the competition between Cu and R sublattices

As $Ho_2Cu_2O_5$, $Yb_2Cu_2O_5$ compound exhibits a low temperature magnetic structure with a non-null propagation vector: in this case $\mathbf{k}=(0,\frac{1}{2},\frac{1}{2})$. Both its magnetic structure [Fig. 6(b) and Table I], and the existence of at least four induced magnetic transitions at 4.2 K under external magnetic field up to 12 T (Ref. 9) suggest a rather high degree of unsatisfied interactions between Cu and Yb sublattices. Consistently, the ordering temperature is the lowest among all $R_2Cu_2O_5$ compounds, and lower than in $Y_2Cu_2O_5$, with only one type of magnetic sublattices.

The neutron-diffraction data show new reflections below $T\approx 8.5$ T (T_{N1}) that can be indexed in the orthorhombic crystal cell with a period $a\times 2b\times 2c$. In particular, this new propagation vector implies that the magnetic periodicity is only recovered after four Cu-O pseudoplanes along c (24.62 Å$=2c$). Despite having 64 magnetic ions in the new cell, the magnetic structure has been solved with the help of symmetry analysis techniques. The magnetic order of Cu and Yb moments is detailed in Table I.

Cu moments inside the crystallographic cell at the origin keep the same arrangement that in $Y_2Cu_2O_5$ and $Er_2Cu_2O_5$, but these $S=\frac{1}{2}$ spins are inverted in neighbor cells along b and c directions. The sequence of Yb moments in the reference chemical unit cell (according to the numbering given in Ref. 8 and Fig. 3) is $(+--+)^{(1)}-(+--+)^{(2)}$ along x, $(+-+-)^{(1)}+(+-+-)^{(2)}$ along y, with null component parallel to z. Figure 1(c) shows the observed and calculated neutron-diffraction patterns of $Yb_2Cu_2O_5$ at 1.5 K. The fit of the five most important magnetic intensities is clearly shown.

A different magnetic structure for $Yb_2Cu_2O_5$ was reported in Ref. 23. By imposing their proposed configuration to fit our data, we only achieve a magnetic R factor of 35% (to be compared to 19.1% from our model). And, moreover, some of the most intense magnetic reflections such as $(1\,\frac{1}{2}\,\frac{3}{2})$ cannot be accurately fitted.

On another hand, we want to emphasize that Yb and Cu sublattices do not order at the same time, in contrast to the rest of members of the family. As a result, the magnetic behavior in $Yb_2Cu_2O_5$ is more complicated than in the other samples studied. The described magnetic structure of $Yb_2Cu_2O_5$ is only stable up to $T_{N1}\approx 8$ K, and the magnetic reflections shown in Fig. 1(c) vanish above that temperature.

The neutron-diffraction data of $Yb_2Cu_2O_5$ reveal that

Cu sublattices order first, at $T_{N2} \approx 13.3$ K. And that the Yb sublattices become ordered through a first-order-like transition only at $T_{N1} \approx 8$ K. In agreement with the heat-capacity measurements reported by Moschalkov *et al.* this intermediate magnetic transition occurs very suddenly.[24] The amplitude of Yb moments becomes saturated in an interval of temperature smaller than ≈ 1 K (the step of the experiment), giving strong evidence of being a first-order phase transition.

The intermediate magnetic regime ($T_{N1} < T < T_{N2}$), between the first-order transition and the paramagnetic state is exceptional in this family of cuprates. As a new evidence of the importance of competing crystal-field and exchange interactions, the copper moments display temperature dependent incommensurate magnetic ordering between T_{N1} and T_{N2}.

Two Bragg magnetic reflections are clearly visible above T_{N1} (we have called them $R1$ and $R2$ in Fig. 8 and Table II). The angles at which they appear vary with temperature between 13 and 8 K, as shown in Table II. The weakness of the magnetic signal makes any further determination very difficult. The magnetic phase transitions are shown in Fig. 8, where the evolution with temperature of the incommensurate reflections is also shown. Let us recall that T_{N2}, as in $Ho_2Cu_2O_5$, coincides with the Néel temperature of $Y_2Cu_2O_5$.

Apparently, unsatisfied Yb-Cu and Cu-Cu interactions are at the origin of the incommensurate arrangement of copper spins in the transitory regime. The Yb-Cu exchange prevents the ordering of Cu moments according to the A mode, and incommensurate magnetic structures arises lowering temperature. Finally, the evolution of ordered Cu spins is frozen at T_{N1}, and the whole magnetic

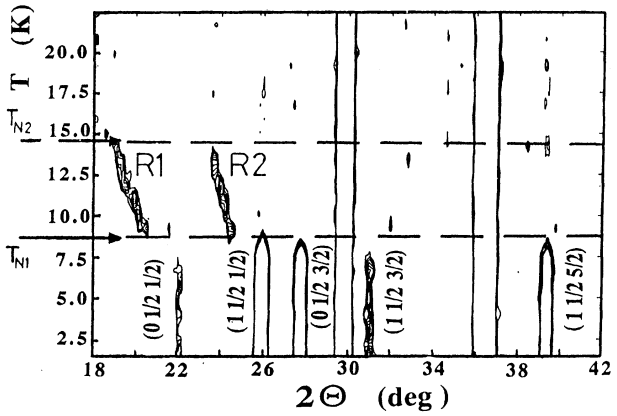

FIG. 8. Isointensity curves of the diffracted neutrons in $Yb_2Cu_2O_5$ as a function of temperature. The two different ordered magnetic regimes are clearly shown: Cu spins display temperature-dependent incommensurate magnetic order between the paramagnetic (above T_{N2}) and the low-temperature (below T_{N1}) regimes. Lowering temperature, Yb moments become abruptly ordered at T_{N1} with their amplitude fully saturated. At this temperature the whole system reacts through a first-order transition, that also involves the transformation of the incommensurate order of Cu spins into the final $\mathbf{k}=(0,\frac{1}{2},\frac{1}{2})$ magnetic structure.

TABLE II. Evolution with temperature of the incommensurable magnetic reflections $R1$ and $R2$ in $Yb_2Cu_2O_5$ in the intermediate regime (see also Fig. 8).

	$R1$		$R2$	
T (K)	2Θ[a] (°)	$\lvert Q\rvert$ (Å^{-1})	2Θ[a] (°)	$\lvert Q\rvert$ (Å^{-1})
9.3	20.4	0.883	24.5	1.058
10.1	20.2	0.874	24.2	1.045
10.9	20.0	0.866	24.1	1.041
11.8	19.5	0.844	24.0	1.037
12.6	19.4	0.840	23.7	1.024
13.4	19.3	0.836	23.7	1.024
14.2	19.1	0.827	23.6	1.020

[a]$\lambda = 2.52$ Å.

system suddenly reacts through a first-order transition. Then, the described magnetic structure with $k=(0,\frac{1}{2},\frac{1}{2})$ is adopted. The final ordering is achieved through a first-order process, since the amplitudes of both Yb and Cu moments are already fully saturated, to 1.4(1) and 1.1(1) μ_B, respectively, at T_{N1}.

IV. CONCLUSIONS

From the analysis of neutron-diffraction data we have determined the magnetic structures of several $R_2Cu_2O_5$ cuprates (R =Y, Er, Tm, Ho, and Yb), ruling out some magnetic arrangements previously proposed. From the combination of magnetization and neutron measurements, magnetic models have been proposed in some cases for the observed field-induced transitions. The overall behavior of this family sheds light to the rare-earth magnetic transitions in superconducting and antiferromagnetic cuprates. In this way, the thermal evolution of $m_R(T)$ is satisfactorily reproduced by a simple model in which the rare-earth moments are polarized under the local effective field from ordered copper spins. The direct R-R interaction seems to be negligible and has no effects on the observed transitions. The complex magnetic behavior found is indicative of crystal-field anisotropy energies being comparable with exchange interactions.

We provide new information upon intermediate magnetic transitions in some samples, and the behavior of copper and rare-earth sublattices as they become magnetically ordered. The intermediate transitions observed in $Ho_2Cu_2O_5$ (commensurate) and $Yb_2Cu_2O_5$ (incommensurate) before the final ordering at temperatures lower than T_N in $Y_2Cu_2O_5$ supports further the idea that the observed propagation vectors express to some extent the degree of frustration, related to unsatisfied interactions in the structure. Low-dimensional ferromagnetic correlations are present along copper chains well above T_N. Finally, our estimations indicate effective Cu-R exchange interactions four times lower than the effective Cu-Cu exchange in the $R_2Cu_2O_5$ structure.

ACKNOWLEDGMENTS

The authors are indebted to Dr. M. Parras, Dr. M. Vallet-Regí, and Dr. J. González-Calbet for supplying the

samples, to Dr. R. Cywinski and Dr. S. H. Kilcoyne for the facilities given to perform some of the measurements, and to the British Council for providing travel funds for these measurements. This research was partially supported by the Spanish CICYT-Midas (Mat: 91-0742), and DGICYT (PB92-0849). The Institut Laue-Langevin is acknowledged for making available the neutron beam time.

[1]J. J. Neumeier, T. Bjornholm, M. B. Maple, and I. K. Schuller, Phys. Rev. Lett. **63**, 2516 (1989).
[2]Y. Dalichaouch, B. W. Lee, C. L. Seaman, J. T. Markert, and M. B. Maple, Phys. Rev. Lett. **64**, 599 (1990).
[3]S. B. Oseroff, D. Rao, F. Wright, D. C. Vier, S. Schultz, J. D. Thompson, Z. Fisk, S. W. Cheong, M. F. Hundley, and M. Tovar, Phys. Rev. B **41**, 1934 (1990).
[4]R. D. Zysler, M. Tovar, C. Rettori, D. Rao, H. Shore, S. Oseroff, Z. Fisk, and S. W. Cheong, Phys. Rev. B **44**, 9467 (1991).
[5]J. T. Markert and B. Jiang, Bull. Am. Phys. Soc. **36**, 982 (1991).
[6]R. L. Fuller and M. Greenblat, J. Solid State Chem. **92**, 386 (1991).
[7]J. F. Bringley, S. Trail, and B. Scott, J. Solid State Chem. **86**, 310 (1990).
[8]J. L. García-Muñoz, J. Rodríguez-Carvajal, X. Obradors, M. Vallet-Regí, J. González-Calbet, and M. Parras, Phys. Rev. B **44**, 4716 (1991).
[9]Z. A. Kazei, N. P. Kolmakova, R. Z. Levitin, B. V. Mill, V. V. Moshchalkov, V. N. Orlov, V. V. Snegirev, and Ja. Zoubkova, J. Magn. Magn. Mater. **86**, 124 (1990).
[10]R. Troć, J. Klamut, Z. Bukowski, R. Horyn, and Stepien-Damm, Physica B **154**, 189 (1989).
[11]J. Rodríguez-Carvajal, FULLPROF: A Program for Rietveld Refinement and Profile Matching Analysis of Complex Powder Diffraction Patterns (ILL, unpublished).
[12]J. L. García-Muñoz, J. Rodríguez-Carvajal, X. Obradors, M. Vallet-Regí, J. González-Calbet, and E. García, Phys. Lett. A **149**, 319 (1990).
[13]J. L. García-Muñoz and J. Rodríguez-Carvajal, J. Solid State Chem. (to be published).
[14]H. R. Freud and H. Müller-Buschbaum, Z. Naturforsch. **32b**, 609 (1977).
[15]E. F. Bertaut, Acta Crystallogr. A **24**, 217 (1968).
[16]G. A. Stewart and J. M. Cadogan, J. Magn. Magn. Mater. **118**, 322 (1993).
[17]G. G. Chepurko, Z. A. Kazei, D. A. Kudrjavtsev, R. Z. Levitin, B. V. Mill, M. N. Popova, and V. V. Snegirev, Phys. Lett. A **157**, 81 (1991).
[18]G. G. Chepurko, I. V. Paukov, M. N. Popova, and Ja. Zoubkova, Solid State Commun. **79**, 569 (1991).
[19]S. W. Cheong, J. D. Thomson, Z. Fisk, K. A. Kubat-Martin, and E. García, Phys. Rev. B **38**, 7013 (1988).
[20]I. V. Golosovsky, V. P. Plakhty, V. P. Harchenkov, S. V. Sharigin, and J. Schweizer, J. Magn. Magn. Mater. (1993).
[21]A. Murasik, P. Fischer, A. Furrer, R. Tro'c, and Z. Bukowski, Physica B **180-181**, 51 (1992).
[22]A. F. Andresen, M. Golab, and A. Szytula, J. Magn. Magn. Mater. **95**, 195 (1991).
[23]A. Murasik, P. Fischer, R. Tro'c, and Z. Bukowski, Solid State Commun. **75**, 785 (1990).
[24]V. V. Moschalkov, N. A. Samarin, Y. Zoubkova, and B. V. Mill, Physica B **163**, 237 (1990).